

## Theory of muon spin relaxation of Mu + CO

Ralph Eric Turner

*Department of Physics, Northwest Community College, 5331 McConnell Avenue, Terrace, British Columbia, Canada V8G 4C2*

R. F. Snider

*Department of Chemistry, University of British Columbia, Vancouver, Canada V6T 1Z1*

(Received 31 July 1997)

In previous papers [Phys. Rev. A **50**, 4743 (1994); **54**, 4815 (1996)] a theoretical description of the signals associated with the muon spin relaxation of simple muonated gaseous radicals has been presented. These gaseous radicals were assumed to have been formed during the slowing down process of the muons in the gaseous target and assumed to be stable chemical species at the initial observation time. The observed signals were attributed to these stable radicals. In this paper the theoretical description is extended to include situations where the radicals are formed in slow processes as opposed to fast processes with the assumption that the muon exists as muonium at the initial observation time. This muonium then reacts for the time duration of the experiment, which is limited by the muon's lifetime. The theoretical treatment is based on an operator expansion of the spin density operators for muonium and for the molecular radicals whose time dependences are described by a set of coupled linearized quantum kinetic equations. Relaxation of the signals is due to two effects, namely, the chemical reactions themselves and the collisions that reorient the molecular radical's rotational angular momentum. This affects the muon's spin via intramolecular couplings between the muon's spin, the radical's free-electron spin, and the radical's rotational angular momentum. The coefficients of the radical's spin Hamiltonian, the collisional reorientation lifetimes (cross sections), and the chemical reaction rates may be used as fitting parameters to describe the experimental signals. These could also be calculated from first principles. [S1050-2947(98)00212-1]

PACS number(s): 36.10.-k, 51.60.+a

### I. INTRODUCTION

Many muon spin relaxation experiments have been performed for the purpose of studying the reactions between the paramagnetic muonium atom (radical),  $\text{Mu} = \mu^+ e^-$ , and macroscopic physical systems [1–3]. For simple molecular gases, these studies fall into general categories depending upon the type of reaction, for example, substitution reactions with diamagnetic molecules such as  $\text{H}_2$  [4] and addition reactions with diamagnetic molecules such as CO [5,6], paramagnetic diatomic molecules such as  $\text{O}_2$  [7] and NO [5,8], and diamagnetic polyatomic molecules such as  $\text{C}_2\text{H}_4$  [9–11]. Often an inert dopant gas is also present to adjust the stopping location of the muons and to ensure that the majority of the muons form the paramagnetic muonium radical that may then react with the molecular gas. For purposes of discussion, the muonium atom will be referred to as a radical to emphasize its chemical reactivity, while paramagnetism and diamagnetism refer to the electronic structure of the atoms and molecules. In these experiments, the dynamics of an ensemble of muon spins are followed through observation of the decay positrons that are emitted preferentially along the muon spin direction. Histograms [12,13] of these ensembles are fitted to a count function

$$N(t) = N_0 e^{-t/\tau_\mu} [1 + S(t)] + B_0, \quad (1)$$

where  $\tau_\mu = 2.2 \mu\text{s}$  is the lifetime of the muon,  $N_0$  is a normalization constant,  $B_0$  is a background constant, and  $S(t)$  is the observed signal. These histograms are recorded with a minimum time resolution of a few nanoseconds and with an

uncertainty in the initial time of a few nanoseconds as well. This uncertainty in the initial time is such that the muons will have completed their stopping process and may be in different chemical environments when counting begins. The count comes from all chemical environments that contain the muon, while the signal  $S(t)$  is related to components of the muon's spin angular momentum  $\mathbf{I}$ . These experiments are usually performed in one of two configurations, namely, a longitudinal setup where the incoming muon's spin and the magnetic field direction  $\hat{\mathbf{B}}$  are collinear and a transverse setup where they are perpendicular. The observed signal  $S(t)$  is proportional to the ensemble-averaged behavior of a single muon's spin time dependence and for computational purposes is calculated as equal to the spin expectation value with the initial incoming state treated in the same way. The result is the same if both the signal and initial state are interpreted as numbers of muons. In general, these signals consist of a number of observable modes having the general forms

$$\begin{aligned} S^L(t) &= \sum_k e^{-\lambda_k^L t} A_k^L + \sum_n e^{-\lambda_n^L t} \cos(\omega_n^L t + \theta_n^L) A_n^L \\ &= \hat{\mathbf{B}} \cdot \langle \mathbf{I} \rangle(t) \end{aligned} \quad (2)$$

for the longitudinal configuration and

$$\begin{aligned} S^T(t) &= e^{-\lambda_0^T t} \sum_k e^{-\lambda_k^T t} \cos(\omega_k^T t + \theta_k^T) A_k^T \\ &= e^{-\lambda_0^T t} \text{Re} \hat{e}_+ \cdot \langle \mathbf{I} \rangle(t) \end{aligned} \quad (3)$$

for the transverse configuration, where  $\hat{e}_+$  is the complex unit vector rotating positively about  $\hat{\mathbf{B}}$ . Here  $\lambda_0^T$  is inversely proportional to the total pressure  $P$ ,

$$\lambda_0^T = \frac{\eta_0}{P}, \quad (4)$$

with  $\eta_0$  being a measured background.  $\lambda_0^T$  contributes to the overall relaxation rate due to field inhomogeneity over the stopping distribution of the muon in the gas [10].

These signals exhibit a variety of frequencies and relaxation rates that may be associated with the different dynamical modes of the chemical system. The relaxation rate for each of the modes is then expressed in terms of the standard terminology for longitudinal  $T_1$  and transverse relaxation times  $T_2$ . When no reactions are present, the relaxation rate, amplitude, and phase of each mode is directly associated with a particular chemical species that contains the muon, provided no accidental degeneracies occur. If chemical reactions are present, the precession-relaxation modes are a composite of all the chemical species since the complex evolution of the chemical dynamics intermixes the contributions of the reorientation rates and spin couplings of all the various chemical environments present. While the frequency of each mode is probably dominated by that of a particular species, shifts occur because of collisions and reactive coupling of the species. In general, there are many modes contributing to these signals, but usually only a single mode is observed experimentally. However, multiple modes have been observed [8,14,15]. For transverse fields, the modes are clearly distinguished by their frequencies so that their relaxation rates and amplitudes may be assigned unambiguously, unless there is a degeneracy. In longitudinal fields, the frequency-dependent modes are usually not observed since their frequencies are too high for the current experimental timing methods to resolve. A further complication for the longitudinal field signals is that more than one zero-frequency mode might be contributing to the observed signal since the relaxation rates may not be sufficiently different to distinguish between the modes. In addition, even in the case when no reactions occur, there is no distinguishing feature to allow the determination of which chemical species is associated with (or dominates) a particular mode.

These experiments may be categorized by the nature of the interactions between the muonium radical and the molecules of the gas. The types of intermolecular processes that occur, such as angular momentum reorientations, spin exchanges, and chemical reactions, lead to a rich precession-relaxation dynamics for the muon's spin. From a theoretical point of view, the categorization may be based on the complexity of the mathematics required to describe the dynamics of the muon's spin angular momentum during the time of data collection. This categorization depends upon the molecular species present and on the partial pressure of the gas. In terms of the intermolecular collisional processes occurring during the time of data collection it is as follows: (i) Chemical reactions involving muonium that produce stable diamagnetic molecules such as  $\text{Mu} + \text{H}_2$  [4], (ii) spin exchange relaxation of muonium by paramagnetic gases such as  $\text{Mu} + \text{Cs}$  [5], (iii) angular momentum reorientation relaxation of stable molecular radicals such as  $\text{MuC}_2\text{H}_4$  in high partial

pressures of  $\text{C}_2\text{H}_4$  [9–11], (iv) chemical reactions involving muonium and diamagnetic gases producing molecular radicals that may undergo angular momentum reorientation relaxations such as  $\text{Mu} + \text{CO}$  [5,6], (v) angular momentum reorientation relaxation and spin exchange of stable molecular radicals such as  $\text{MuO}_2$  in high partial pressures of  $\text{O}_2$  [7], and (vi) chemical reactions involving muonium and paramagnetic gases producing molecular radicals that may undergo angular momentum reorientation relaxation and spin exchange such as  $\text{Mu} + \text{O}_2$  in low partial pressures of  $\text{O}_2$  [7]. Theoretical descriptions of categories (i) [4,5], (ii) [16–18], and (iii) [19–21] have already been presented, while it is the purpose of the present paper to present a theoretical perspective on category (iv). In all these categories, there are two types of dynamical motion occurring, that is, the intramolecular evolution of all the translational and internal degrees of freedom of the molecules and radicals and the intermolecular collisional events between these atoms and molecules. Since the observable of interest is the muon's spin angular momentum, the translational degrees of freedom are averaged over in both the experiments and the theory. Thus the theoretical problem involves the free (between collisions) spin dynamics of the molecules and radicals coupled by the collisional reaction and relaxation processes, with the result that the observed muon spin signal has a relaxation of its amplitude and possibly indirect shifts of the observed frequencies from the free intramolecular frequencies. Relaxation of the signals is due to the collision events that may or may not directly relax the muon's spin angular momentum  $\mathbf{I}$ . The resulting equations for the dynamical motion of the internal degrees of freedom of the molecules and radicals containing the muon are affected by collisions via angular momentum reorientation cross sections, spin exchange cross sections, and chemical reaction rates. Solution of equations of this type result in signals of the forms of Eqs. (2) and (3) where the observable frequencies, relaxation rates, amplitudes, and phases are, in general, dependent both upon the internal state properties of the molecules and the radicals, as well as on the reorientation, spin exchange, and chemical reaction collision cross sections. These are in turn dependent on the pressure and magnetic field strength.

For category (i), the muon completes its slowing down process as the muonium radical and then reacts with a diamagnetic gas molecule [4] after counting begins. In longitudinal fields only the zero-frequency signals are observed, while for transverse fields only the two lowest muonium frequencies and the diamagnetic (or bare muon) frequency are observed. The reaction is assumed to be thermal with a chemical reaction rate that is observable on the time scale of the experiments, a few nanoseconds to about 10  $\mu\text{s}$ . The products of this type of reaction, for example,



are stable diamagnetic molecules such as  $\text{MuH}$ . Relaxation of the signal occurs due to loss of muonium through the chemical reaction as the muonium is converted to the diamagnetic molecule. There are no other relaxation methods for these types of experiments. The free intramolecular spin

dynamics of the diamagnetic molecule involves only the spin angular momentum of the muon  $\mathbf{I}$  and the magnetic field  $\mathbf{B}$  in the Zeeman Hamiltonian

$$H_{\mu}^{\text{sp}}/\hbar = -\omega_{\mu}\hat{\mathbf{B}}\cdot\mathbf{I}, \quad (6)$$

while the muonium radical also involves the spin of the electron  $\mathbf{S}$ . The spin Hamiltonian for muonium is the standard hydrogen isotope Hamiltonian [3,22–24] constructed from the electron spin angular momentum, the muon spin angular momentum, and the external magnetic field as

$$H_{\text{Mu}}^{\text{sp}}/\hbar = \omega_e\hat{\mathbf{B}}\cdot\mathbf{S} - \omega_{\mu}\hat{\mathbf{B}}\cdot\mathbf{I} + \omega_0^{\text{Mu}}\mathbf{S}\cdot\mathbf{I}. \quad (7)$$

This standard muonium or hydrogen spin Hamiltonian has well known analytic eigenfunctions and eigenvectors [25]. Those modes that influence the muon signal are three zero-frequency and two nonzero-frequency longitudinal modes and four nonzero-frequency transverse modes. With the current experimental apparatuses, only the two lower nonzero frequency transverse modes are observable as well as the sum of the zero-frequency longitudinal modes. Because of the simplicity of the free spin dynamics and the averaging over the translational degrees of freedom, it is possible to analytically represent the signals for this category [4,5].

In the longitudinal field experiments [5] when there are only forward reactions, the zero frequency contribution to the signal from muonium is

$$S_{\text{Mu}}^L(t) = \frac{1}{2}e^{-\lambda_f t}[1 + \cos^2\eta]f_{\text{Mu}}\langle I_B \rangle_{\mu}(0), \quad (8)$$

while the zero-frequency contribution to the signal from the diamagnetic environment is

$$S_D^L(t) = \frac{1}{2}[1 - e^{-\lambda_f t}][1 + \cos^2\eta]f_{\text{Mu}}\langle I_B \rangle_{\mu}(0) + f_D\langle I_B \rangle_{\mu}(0), \quad (9)$$

with

$$\cos\eta = \frac{x}{\sqrt{1+x^2}}. \quad (10)$$

Here  $\lambda_f = k_f n_X$  is the rate due to the forward reaction, with  $n_X$  being the number density of the reacting gas, and  $x = B/B_0$  is the reduced magnetic field strength.  $B_0$  is  $\omega_0^{\text{Mu}}/(\gamma_e + \gamma_{\mu}) = 1585$  G.  $\langle I_B \rangle_{\mu}(0)$  is the muon spin expectation value in the field direction of the incoming muon beam at the zero of the count time, which is usually indistinguishable from the time when the muon is thermalized.  $f_{\text{Mu}}$  and  $f_D$  are the initial (zero of count time  $f_{\text{Mu}} + f_D \leq 1$ ) fractions for the muonium and diamagnetic chemical environments. This diamagnetic environment plays no further role in the chemical or spin relaxation processes. In the experiments, these contributions to the signal cannot be individually identified and only the sum of terms from muonium and from the diamagnetic environment can be observed, that is,

$$S^L(t) = S_{\text{Mu}}^L(t) + S_D^L(t) = A_1 = \left\{ \frac{1}{2}[1 + \cos^2\eta]f_{\text{Mu}} + f_D \right\} \langle I_B \rangle_{\mu}(0); \quad (11)$$

compare with Eq. (2). Thus there is only one observed zero-frequency mode that does not relax. It is to be noted that the amplitude of this constant signal increases with field and contains contributions from all the chemical environments. This is the typical result for the forward reaction from muonium to a diamagnetic molecule in longitudinal fields.

In transverse fields the experiments [4,5] are often carried out at low fields ( $\leq 10$  G). For such low transverse fields and for only forward reactions, the signal is calculated as the expectation value of the muon spin in the  $\hat{\mathbf{x}}$  direction, which is a direction perpendicular to the magnetic field direction  $\hat{\mathbf{B}}$ . The initial state is interpreted in the same way as for the longitudinal case, while the muonium contribution to the signal is

$$S_{\text{Mu}}^T(t) = \frac{1}{2}e^{-\lambda_f t} \cos(\omega_{\text{Mu}}t) f_{\text{Mu}} \langle I_x \rangle_{\mu}(0) \quad (12)$$

and the diamagnetic contribution to the signal is

$$S_D^T(t) = \cos(\omega_{\mu}t) f_D \langle I_x \rangle_{\mu}(0) + \frac{1}{2} \cos\theta [\cos(\omega_{\mu}t - \theta) - e^{-\lambda_f t} \cos(\omega_{\text{Mu}}t + \theta)] f_{\text{Mu}} \langle I_x \rangle_{\mu}(0). \quad (13)$$

Here  $\omega_{\text{Mu}}$  is the low-field effective Zeeman precession frequency  $(\omega_e - \omega_{\mu})/2$ ,  $\lambda_f$  is the chemical reaction relaxation rate, and the phase is

$$\theta = \arctan \left[ \frac{\omega_{\text{Mu}} + \omega_{\mu}}{\lambda_f} \right]. \quad (14)$$

This phase depends upon pressure through the rate  $\lambda_f$  and the field through the precession frequencies  $\omega_{\text{Mu}}$  and  $\omega_{\mu}$ . As with the longitudinal signal, these contributions to the signal cannot be individually identified and only the sum of the contributions from both the muonium and the diamagnetic environments can be observed, that is,

$$S^T(t) = A_0 \cos(\omega_{\mu}t + \theta_0) + e^{-\lambda_f t} A_1 \cos(\omega_{\text{Mu}}t + \theta_1), \quad (15)$$

where the amplitudes and phases for the modes are

$$A_0 = \sqrt{\left[ \frac{1}{2}f_{\text{Mu}} + f_D \right]^2 \cos^2\theta + f_D^2 \sin^2\theta} \langle I_x \rangle_{\mu}(0),$$

$$\theta_0 = -\arctan \left\{ \frac{\frac{1}{2}f_{\text{Mu}} \tan\theta}{\left( \frac{1}{2}f_{\text{Mu}} + f_D \right) + f_D \tan^2\theta} \right\}, \quad (16)$$

$$A_1 = \frac{1}{2}(\sin\theta) f_{\text{Mu}} \langle I_x \rangle_{\mu}(0),$$

$$\theta_1 = \theta - \pi/2.$$

Thus there are two nonzero-frequency modes; compare with Eq. (3). The amplitudes of these modes are pressure and field dependent. Only the second mode relaxes and its relaxation rate is equal to the chemical reaction rate  $\lambda_1 = \lambda_f$ . In this example, the first mode is due to both the initial diamagnetic fraction and the diamagnetic product of the chemical reaction, which may not necessarily be the same chemical environment. In addition, even though the second mode has the muonium frequency, it contains contributions from both muonium and the diamagnetic product of the chemical reaction.

If this reaction is reversible, the effect of the reverse reaction will show up as modifying the frequencies, relaxation rates, and amplitudes of the observed modes under standard chemical kinetic conditions [5]. For example, in longitudinal fields, the zero frequency contribution to the signal from muonium is

$$S_{\text{Mu}}^L(t) = \left\{ \left[ \frac{\lambda_r - \lambda_1}{\lambda_2 - \lambda_1} \right] e^{-\lambda_1 t} + \left[ \frac{\lambda_2 - \lambda_r}{\lambda_2 - \lambda_1} \right] e^{-\lambda_2 t} \right\} \times \frac{1}{2} [1 + \cos^2 \eta] f_{\text{Mu}} \langle I_B \rangle_{\mu}(0), \quad (17)$$

while the zero-frequency contribution to the signal from the diamagnetic environment is

$$S_D^L(t) = f_D \langle I_B \rangle_{\mu}(0) + \left[ \frac{\lambda_f}{\lambda_2 - \lambda_1} \right] [e^{-\lambda_1 t} - e^{-\lambda_2 t}] \times \frac{1}{2} [1 + \cos^2 \eta] f_{\text{Mu}} \langle I_B \rangle_{\mu}(0). \quad (18)$$

Here the relaxation rates are

$$\lambda_1 = \frac{\lambda_f + \lambda_r}{2} - \frac{1}{2} \sqrt{\lambda_f^2 + 2\lambda_f \lambda_r \cos^2 \eta + \lambda_r^2}, \quad (19)$$

$$\lambda_2 = \frac{\lambda_f + \lambda_r}{2} + \frac{1}{2} \sqrt{\lambda_f^2 + 2\lambda_f \lambda_r \cos^2 \eta + \lambda_r^2}.$$

Again these contributions cannot be individually identified and it is only the sum of these contributions that is observed, that is,

$$S^L(t) = A_0 + e^{-\lambda_1 t} A_1 + e^{-\lambda_2 t} A_2, \quad (20)$$

where the amplitudes of the observed modes are now

$$A_0 = f_D \langle I_B \rangle_{\mu}(0),$$

$$A_1 = \left[ \frac{\lambda_2}{\lambda_2 - \lambda_1} \right] \frac{1}{2} [1 + \cos^2 \eta] f_{\text{Mu}} \langle I_B \rangle_{\mu}(0), \quad (21)$$

$$A_2 = \left[ \frac{-\lambda_1}{\lambda_2 - \lambda_1} \right] \frac{1}{2} [1 + \cos^2 \eta] f_{\text{Mu}} \langle I_B \rangle_{\mu}(0);$$

compare with Eq. (2). This observable signal consists of three zero-frequency modes, two of which have pressure- and field-dependent amplitudes and relaxation rates. One of these rates will be slow and the other fast. As the field in-

creases,  $A_1$  increases,  $A_2$  decreases,  $\lambda_1 \rightarrow 0$ , and  $\lambda_2$  increases. This implies that at large fields the signal will be constant.

For category (ii), the interaction between the paramagnetic muonium radical and a paramagnetic gas, for example, Cs [5], is dominated by electron spin exchange processes whereby the spin angular momentum of the electron in the muonium directly interacts with the paramagnetic spin angular momentum of a gas molecule in a collision process. While the muon spin will also directly interact with the gas molecule's paramagnetic spin, the size of this interaction is much smaller than that of the electron's interaction and this direct interaction can be ignored; see the successful theoretical description of this process in [16]. Thus the relaxation of the muon's spin angular momentum by spin exchange interactions is indirect. Specifically, whereas the muonium's electron spin angular momentum is directly relaxed due to collisional couplings with the paramagnetic spin, the relaxation of the muon's spin occurs only because the muon and electron spins are strongly coupled in the intramolecular spin dynamics of the muonium radical. The relaxation rates may be expressed in terms of spin exchange collision cross sections or, equivalently, collision lifetimes. In this manner, the detailed spin dynamics of the muonium radical is modified by the direct relaxation of the electron's spin. However, the description of the spin dynamics still only involves the spins  $\mathbf{S}$  and  $\mathbf{I}$  since the effects of the spins of the paramagnetic gas molecules appear only in the collision cross sections. For certain ranges of magnetic fields, the signals can be expressed in analytic terms [16]. In particular, for the zero-frequency longitudinal experiment, there are two modes, one that does not relax and is due to the initial diamagnetic fraction and one that has an exponential decay whose relaxation rate (which depends upon both the spin exchange lifetime  $\tau$  and the magnetic field) goes to zero for high fields,

$$S^L(t) = A_0 + e^{-\lambda_1 t} A_1,$$

$$A_0 = f_D \langle I_B \rangle_{\mu}(0), \quad (22)$$

$$A_1 = \frac{1}{2} [1 + \cos^2 \eta] f_{\text{Mu}} \langle I_B \rangle_{\mu}(0),$$

$$\lambda_1 = \sin^2 \eta / 2\tau.$$

In low-field ( $\leq 10$  G) transverse experiments, there are also two modes, one of which has an exponential decay whose rate is determined by the spin exchange lifetime, namely,

$$S^T(t) = A_0 \cos(\omega_{\mu} t) + e^{-\lambda_1 t} A_1 \cos(\omega_{\text{Mu}} t),$$

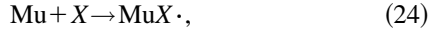
$$A_0 = f_D \langle I_x \rangle_{\mu}(0), \quad (23)$$

$$A_1 = \frac{1}{2} f_{\text{Mu}} \langle I_x \rangle_{\mu}(0),$$

$$\lambda_1 = 1/2\tau.$$

For categories (iii) and (iv), the interaction between the paramagnetic muonium radical and the diamagnetic gas is dominated by chemical reactions. Since the gas is diamagnetic, no spin exchange processes occur. The distinction between these categories depends upon whether the reactions

are fast or slow with respect to when the experimental counting begins. When the incoming muons slow down in the gas, muonium is produced at high energies through a series of charge exchange processes [13,26]. Further chemical reactions with the gas may occur under either fast or slow conditions on the time scale of the slowing down process. For category (iii) (fast processes),



the radical  $\text{MuX}\cdot$  is formed before the slowing down process is complete and the first count begins. If this radical is stable during the lifetime of the muon, then the observed signal will be due solely to the radical. Such a situation exists for the radicals  $\text{C}_2\text{H}_4\text{Mu}\cdot$  and  $\text{C}_2\text{D}_4\text{Mu}\cdot$  [9–11] when their partial pressures are large enough. A detailed theoretical treatment, with fitting to the experimental data for the former, has been presented by the current authors; see Refs. [19,20]. The chemical reactions are completed before the radical signal is observed and thus do not contribute to the observed relaxation. As for  $\text{C}_2\text{H}_4\text{Mu}\cdot$ , the relaxation of the signal is indirect, being due to the coupling of the muon's spin angular momentum with other angular momenta, which are in turn relaxed by reorientation collisions. In order that a theoretical treatment be tractable, it was necessary to make some set of assumptions about the radical. These assumptions deal with the free evolution of the radical and its angular momentum properties since it is the dynamical motion of the coupled spin system while the radical is in free flight between collisions that presents the major difficulty in a theoretical treatment. The radical has an electron spin  $\mathbf{S}$ , a muon spin  $\mathbf{I}$ , possibly other nuclear spins as well as a rotational angular momentum  $\mathbf{J}$ , and various vibrational, bending, and torsional degrees of freedom. To include all of these dynamical quantities, which are all expected to be coupled, would lead to an extremely large basis set and also to the question of whether the experimental data are either accurate enough or sufficient to uniquely determine all the coupling constants in the Hamiltonian and the collisional decay times required to parametrize all these quantities. A reduction in the size of the basis set was required and it was assumed that not all the quantities would be important for the bulk phase relaxation. Three assumptions were made about the dynamics. First was that the bending, vibrational, and torsional degrees of freedom could be ignored since they are too high in energy to substantially contribute to the motion. Second, for the cases considered so far, the radical has been approximated as a diatomic molecule as far as its rotational motion is concerned. Furthermore, the effects of the rotational angular momentum were assumed to be well approximated by using a single average magnitude  $J$  since this is large. In addition, a multipole expansion in  $\mathbf{J}$  was carried out and truncated at second order. Finally, the third assumption was that all other nuclear spins, such as protons, may be ignored since the largest coupling of the muon spin is to the electron's spin. Thus the spin Hamiltonian for the radical is constructed from the angular momenta  $\mathbf{S}$ ,  $\mathbf{J}$ , and  $\mathbf{I}$  and the external magnetic field  $\mathbf{B}$  as

$$H_{\text{MuX}}^{\text{SP}}/\hbar = \omega_e \hat{\mathbf{B}} \cdot \mathbf{S} - \omega_\mu \hat{\mathbf{B}} \cdot \mathbf{I} + \omega_0^{\text{MuX}} \mathbf{S} \cdot \mathbf{I} - \omega_J^{\text{MuX}} \hat{\mathbf{B}} \cdot \mathbf{J} + \omega_{\text{SR}}^{\text{MuX}} \mathbf{S} \cdot \mathbf{J} + \omega_{\text{IR}}^{\text{MuX}} \mathbf{I} \cdot \mathbf{J} + c_A^{\text{MuX}} \mathbf{I} \cdot [\mathbf{J}]^{(2)} \cdot \mathbf{S}. \quad (25)$$

The free evolution of the spin dynamics for this category of systems are much more complex than those of categories (i) and (ii). This approach has been successfully used [20] to globally fit both the longitudinal and transverse signals for the radical  $\text{C}_2\text{H}_4\text{Mu}\cdot$ . In each of the longitudinal and transverse field configurations, only one relaxation mode has been observed. For both of these cases, the relaxation rates depend upon the field and pressure.

In category (iv), the muons complete their stopping as muonium radicals before the first count and then react to form a metastable paramagnetic radical during the time of experimental observation



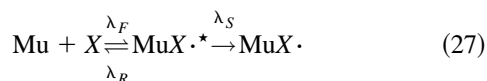
where, for example,  $X = \text{CO}$  [5,6]. The addition reaction may be reversible since the product may be an excited state of the radical or a metastable radical. Further reaction of  $\text{MuX}\cdot^*$  may occur to produce a stable radical. As in category (iii), the muon's spin is indirectly relaxed, being dominated by the coupling of the muon's spin to other angular momenta of the radical, which are in turn directly relaxed by collisions, including chemical reactions. Thus category (iv) involves adding the complexity of chemical reactions to the spin dynamics of category (iii). For carbon monoxide and transverse fields, only signals associated with the muonium frequencies have been observed, while no signal having a radical frequency has been seen [5,6,27]. If these reactions were reversible, the effect of the reverse reactions should show up by modifying the decay rates and amplitudes of the signals associated with the muonium frequencies. A further complexity is that the muonium frequencies may be shifted since collisions can modify (indirectly) the effective coupling between the spins. Properties of the radical must then be deduced from measurements of these quantities. Deducing properties from the longitudinal signals is even more complex since there are several zero-frequency modes and the observed longitudinal signal may have major contributions from a number of these as well as from the different chemical species that are present. With a finer time resolution it might be possible to observe the frequency-dependent modes of the molecular radicals in the longitudinal experiments, which would be of great help in analyzing the dominant features of the reacting, precessing system. Analytic solutions for the amplitudes and relaxation rates are not possible for either of these categories.

Finally, for categories (v) and (vi), spin exchange collisional effects must be added to the chemical and rotational dynamics of categories (iii) and (iv). The present treatment does not include these effects.

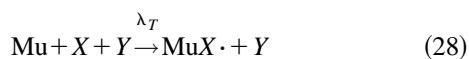
In Sec. II the coupled quantum kinetic equations for muonium and the radicals are considered, appropriate for the category (iv) system  $\text{Mu} + \text{CO}$ . The operator bases for the longitudinal and transverse signals are presented in Sec. III, while the observable signals are discussed in Sec. IV. A preliminary fit of the presently available data is given in Sec. V.

## II. CHEMICAL REACTIONS AND KINETIC EQUATIONS

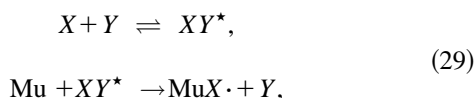
The chemical reactions of interest are the formation of molecular radicals by collisions between muonium radicals and gas molecules through second-order



and third-order



reaction schemes. For the second-order reaction scheme the forward, reverse, and stabilization chemical rates for the metastable radical are  $\lambda_F$ ,  $\lambda_R$ , and  $\lambda_S$ , respectively, while for the third-order reaction scheme the rate of formation of the radical is  $\lambda_T$ . These reaction schemes involve the muonium radical, a metastable molecular radical  $\text{MuX} \cdot^*$ , and a stable radical  $\text{MuX} \cdot$ . The gas is assumed to consist of two species:  $X$ , which is reactive, and  $Y$ , which forms a nonreactive background. When no distinction between the gas molecules is required, the general notation  $Z$  will be used. In the second-order reaction scheme, the muonium radical and a reactive gas molecule collide to form the metastable radical, which may undergo unimolecular decay back to the reactants or may collide with another gas molecule  $Z$  to form the stable radical. This metastable complex is presumably either a long-lived resonant or orbiting state. The second reaction scheme could be associated with the detailed mechanism,



involving the formation of the radical through a standard two-step bimolecular collision process. First, the reactant and nonreactant gas molecules are assumed to form complexes through binary collisions. Then this complex undergoes a binary collision with muonium, resulting in an exchange reaction producing a stable radical. Since both  $X$  and  $Y$  species are present in the gas before a muon is injected into the system, there should be an equilibrium concentration of such  $XY$  complexes, which should be appreciable at the high pressures involved in many of the experiments. That the third-order formation of the radical is important is determined by its need for fitting the experimental data. That is, without the presence of this pathway, reasonable fits to the data are not obtained, whereas with the inclusion of this mechanism reasonable fits are obtained.

The pseudo-first-order chemical rate constants for these second- and third-order reaction schemes are thus functions of the concentrations of the respective species according to

$$\begin{aligned} \lambda_F &= k_{fb} n_X, & \lambda_T &= k_{f1} n_X n_Y, \\ \lambda_R &= k_r, & \lambda_S &= k_s n_{\text{tot}}. \end{aligned} \quad (30)$$

While these reaction schemes involve specific second- and third-order rates, the spin dynamics is expressed in terms of the chemical species present. In particular, there will be loss  $L$  and gain  $G$  rates for each chemical species, that is,

$$\begin{aligned} \lambda_{\text{Mu}}^L &= \lambda_F + \lambda_T, \\ \lambda_{\text{Mu}}^G &= \lambda_R, \end{aligned}$$

$$\lambda_{\text{MuX} \cdot^*}^L = \lambda_R + \lambda_S, \quad (31)$$

$$\lambda_{\text{MuX} \cdot^*}^G = \lambda_F,$$

$$\lambda_{\text{MuX} \cdot}^G = \lambda_T + \lambda_S,$$

and there is no chemical loss for the stable radical. These chemical rates may now be related to the spin dynamics through a set of coupled kinetic equations.

The spin dynamics is described by three coupled quantum linear kinetic equations [28–30], one for each chemical species. This motion is generated by four different processes, namely, the free (between collision) spin dynamics of the chemical species, the reorientation collisions that indirectly relax the radical spins, the chemical reactions that result in the loss of a chemical species, and the chemical reactions that produce a chemical species. Between one collision and another, the spin dynamics for a species is determined by a Liouville superoperator  $\mathcal{L}$ . When the chemical processes are bimolecular, the collision effects causing reorientational relaxation and chemical loss are described by collision superoperators  $\mathcal{R}$  for the collision processes, whose detailed form is the same as for the linear Boltzmann equation. The bimolecular production or gain processes that create new chemical species are also described by collision superoperators  $\mathcal{P}$  of Boltzmann equation form. In contrast, a unimolecular process requires a different form for its dynamic superoperator. The resulting kinetic equations are put into matrix form by using appropriate spin operator bases.

Since there is only one muon in the gas at a time, the muon is passed from one species to another and the remainder of the gas is in thermal equilibrium. Thus the kinetic equations are linear in the deviation from equilibrium. Moreover, since the observable of interest is the muon spin angular momentum, the translational degrees of freedom may be averaged over with the appropriate Maxwellians. The coupled equations for the spin density operators thus become

$$\begin{aligned} \frac{\partial \rho_{\text{Mu}}^{\text{sp}}(t)}{\partial t} + i \mathcal{L}_{\text{Mu}}^{\text{sp}} \rho_{\text{Mu}}^{\text{sp}}(t) &= \mathcal{P}_{\text{Mu}, \text{MuX} \cdot^*}^{\text{sp}} \rho_{\text{MuX} \cdot^*}^{\text{sp}}(t) - \mathcal{R}_{\text{Mu}} \rho_{\text{Mu}}^{\text{sp}}(t), \\ \frac{\partial \rho_{\text{MuX} \cdot^*}^{\text{sp}}(t)}{\partial t} + i \mathcal{L}_{\text{MuX} \cdot^*}^{\text{sp}} \rho_{\text{MuX} \cdot^*}^{\text{sp}}(t) &= \mathcal{P}_{\text{MuX} \cdot^*, \text{Mu}}^{\text{sp}} \rho_{\text{Mu}}^{\text{sp}}(t) \\ &\quad - \mathcal{R}_{\text{MuX} \cdot^*} \rho_{\text{MuX} \cdot^*}^{\text{sp}}(t), \quad (32) \\ \frac{\partial \rho_{\text{Mu}}^{\text{Xsp}}(t)}{\partial t} + i \mathcal{L}_{\text{MuX}}^{\text{sp}} \rho_{\text{MuX}}^{\text{sp}}(t) &= \mathcal{P}_{\text{MuX}, \text{MuX} \cdot^*}^{\text{sp}} \rho_{\text{MuX} \cdot^*}^{\text{sp}}(t) \\ &\quad + \mathcal{P}_{\text{MuX}, \text{XY} \cdot}^{\text{sp}} \rho_{\text{Mu}}^{\text{sp}}(t) \\ &\quad - \mathcal{R}_{\text{MuX}} \rho_{\text{MuX}}^{\text{sp}}(t), \end{aligned}$$

where the molecular spin Liouville superoperator  $\mathcal{L}^{\text{sp}}$  for each species is defined in terms of the relevant spin Hamiltonian by

$$\mathcal{L}^{\text{sp}} A \equiv (1/\hbar) [H^{\text{sp}}, A]_- . \quad (33)$$

For bimolecular events, the linearized relaxation superoperator  $\mathcal{R}$  for species  $\alpha$  involves the traces  $\text{Tr}^{\text{tr}}$  over the transla-

tional states of the colliding pair of molecules and the trace  $\text{Tr}_Z^{\text{int}}$  over any internal states of the reacting gas molecules (species  $Z$ ), of the transition superoperator  $\mathcal{T}_{\alpha,Z}$  acting on the spin density operator  $\rho_\alpha^{\text{sp}}$  of species  $\alpha$ , and weighted by the product of Maxwellian density operators  $\rho^{\text{mom}}$  for each colliding species. Incorporating a sum over all the background gases with  $n_Z$  denoting the density of background gas  $Z$ , a typical spin relaxation superoperator is formally

$$\begin{aligned} \mathcal{R}_\alpha \rho_\alpha^{\text{sp}} &= \sum_Z n_Z \text{Tr}_Z^{\text{int}} \text{Tr}_\alpha^{\text{tr}} \text{Tr}_Z^{\text{tr}} i \mathcal{T}_{\alpha,Z} [\rho_Z^{\text{mom}} \rho_\alpha^{\text{mom}} \rho_Z^{\text{int}} \rho_\alpha^{\text{sp}}] \\ &= \lambda_\alpha \rho_\alpha^{\text{sp}}. \end{aligned} \quad (34)$$

The last line of this equation denotes the parametrization of the processes assumed in this work. Both chemical reaction and reorientation processes are included in these relaxation superoperators and the relaxation rates  $\lambda_\alpha$  are appropriate for the processes involving species  $\alpha$ . For the production processes  $\mathcal{P}$ , these are of three types. The formation of the stable radical from the metastable is clearly of bimolecular type and so has the formal structure, for species  $\alpha \neq \beta$ ,

$$\begin{aligned} \mathcal{P}_{\alpha,\beta} \rho_\beta^{\text{sp}} &= \sum_Z n_Z \text{Tr}_Z^{\text{int}} \text{Tr}_\alpha^{\text{tr}} \text{Tr}_Z^{\text{tr}} (-i) \mathcal{T}_{\alpha,\beta,Z} [\rho_Z^{\text{mom}} \rho_\beta^{\text{mom}} \rho_Z^{\text{int}} \rho_\beta^{\text{sp}}] \\ &= \lambda_{\alpha,\beta} \rho_\beta^{\text{sp}}. \end{aligned} \quad (35)$$

In contrast, for the unimolecular decay, it is inappropriate to formulate this process in the same way as above. A detailed analysis of how to mathematically formulate this will not be attempted here, but it should be recognized that this process is just part of the continuing evolution of the interacting molecular fragments. What is of interest for this work is what happens to the spin, including the molecular rotation, during formation and breakup of the metastable radical. In this work this is modeled as a simple overlap of the spin state before and after the reaction. When there are two fragments, each carrying some angular momentum polarization, the spin state is taken as the product of the spin states of the two fragments.

For the collision superoperators describing relaxation, it is assumed in the following that the collision superoperator acts only on the rotational motion of the molecule, specifically not on either the muon or electron spins. This is based on the rationale that the muon and electron spins do not inherently play a direct role in the collision process and so their states should remain unchanged during the collision process. A similar argument for reactive collisions implies that the spin states are passed directly from the reactant to the product with no change. These assumptions will be expressed quantitatively after appropriate basis sets for the spin systems are presented.

To numerically solve the set of coupled rate equations (32), it is convenient to embed all the spin density operators for the species containing the muon, namely, for the muonium radical, the metastable molecular radical, and the stable molecular radical, into one large operator space

$$\rho(t) = \rho_{\text{Mu}}^{\text{sp}}(t) \oplus \rho_{\text{MuX}^*}^{\text{sp}}(t) \oplus \rho_{\text{MuX}}^{\text{sp}}(t). \quad (36)$$

This combined density operator satisfies an evolution equation

$$\frac{\partial \rho(t)}{\partial t} = -\mathcal{G} \rho(t), \quad (37)$$

whose time dependence is determined by a motion generator

$$\mathcal{G} = \mathcal{R} - \mathcal{P} + i\mathcal{L}, \quad (38)$$

consisting of the direct sum of the individual spin dynamical Liouville and relaxation superoperators for each species, together with production superoperators between the individual species.

### III. BASIS SETS

In order to reduce the reaction-precession equation (37) to matrix form for its solution, it is necessary to introduce appropriate operator basis sets for each species. The motion generator must then be determined in this basis. Since it is the vector operator  $\mathbf{I}$  that is to be observed, it is sufficient to restrict the operator bases to vector-valued combinations of the vectors describing the spin system. The latter consist of the spin operators and the magnetic field direction  $\hat{\mathbf{B}}$ . For the muonium radical, the vector basis is 16 dimensional, while each of the molecular radicals has 95 elements (if the rotational multipole expansion is truncated at second order). Thus, to include all three radicals, the full combined basis set would have 206 (16+95+95) elements, with the first 16 being muonium, the next 95 the metastable radical, and the last 95 the stable radical. Structurally, the muonium radical's free motion generator lies in the first 16×16 diagonal block, the metastable molecular radical's free motion (Liouville) generator in the next 95×95 diagonal block, and the stable molecular radical's in the final 95×95 block of the generator matrix. Reorientation rates for the molecular radicals will lie in the respective 95×95 blocks and cause direct relaxation of the spins of their respective radicals. In contrast, the chemical reaction gain rates couple the different blocks, while the chemical reaction loss terms again lie within the appropriate diagonal blocks. As a non-Hermitian matrix, the eigenvalues are complex. These are to be determined, together with their associated eigenvectors, and used to calculate longitudinal and transverse signals for comparison with experiment. However, symmetry can simplify the calculations. Specifically, the presence of the magnetic field implies that the spin system satisfies  $C_{\infty v}$  symmetry and the vector valued bases split into longitudinal and transverse subbases. The latter further split into counterclockwise (+) and clockwise (−) rotating bases. This was the method used in Refs. [19,20] for the  $\text{C}_2\text{H}_4\text{Mu}\cdot$  problem and is used in the current description. The block nature of the motion generator in the full basis carries directly over into the reduced bases.

The general, vector-valued, operator basis set for a molecular radical was described in Refs. [19,20], together with the evaluation of the motion generator in this basis. The reduction to the longitudinal and transverse basis sets were extracted by selecting out particular scalar components of the vector valued basis. The details of this reduction are given in Refs. [19,20]. Here only the longitudinal and counterclockwise transverse bases are explicitly discussed, with the ex-

press purpose of calculating the matrices that describe the chemical reactions.

### A. Longitudinal basis set

When reduced to the longitudinal configuration, the basis  $\Phi_N$  [19,20] consists of 75 elements: 5 for muonium, 35 for the metastable radical, and 35 for the stable radical. The

$$\Phi_N = \sqrt{2\alpha + 1} \mathcal{Y}^{(n)}(\mathbf{J}) \mathcal{Y}^{(m)}(\mathbf{S}) \odot^{m+n} \mathbf{V}(m, n, \alpha) \odot^\alpha \mathbf{V}(\alpha, p, r) \odot^{p+r} \mathcal{Y}^{(r)}(\hat{\mathbf{B}}) \mathcal{Y}^{(p)}(\mathbf{I}), \quad 6 \leq N \leq 40. \quad (39)$$

The stable radical basis elements will have the same form, but the numbering is  $41 \leq N \leq 75$ . The notation for irreducible Cartesian tensors  $\mathcal{Y}^{(n)}$ ,  $n$ -fold tensor contraction  $\odot^{(n)}$ , and Clebsch-Gordan tensors  $\mathbf{V}(m, n, \alpha)$  follows that of Coepe and Snider [31,32]. These operators form part of the 75-dimensional basis that is orthonormal with respect to the inner product

$$\langle\langle Y|Z \rangle\rangle \equiv \frac{1}{4\pi(2I+1)(2S+1)(2J+1)} \text{Tr}_{I,S,J} \int d\hat{\mathbf{B}} Y^\dagger Z. \quad (40)$$

For each molecular radical, the numerical index  $N$  is used to classify, in some convenient order, the set of parameters  $mnp\alpha$  [20].

For muonium, the basis requires only the coupling of the electron's spin  $\mathbf{S}$ , the muon's spin  $\mathbf{I}$ , and the magnetic field direction  $\hat{\mathbf{B}}$ , which is a special case of Eq. (39),

$$\Phi_N = \mathcal{Y}^{(m)}(\mathbf{S}) \odot^m \mathbf{V}(m, p, r) \odot^{r+p} \mathcal{Y}^{(r)}(\hat{\mathbf{B}}) \mathcal{Y}^{(p)}(\mathbf{I}), \quad 1 \leq N \leq 5. \quad (41)$$

$N$  is an index for this portion of the basis referring to the indices  $m$ ,  $p$ , and  $r$ , which represent the tensorial nature of the electron spin, the muon spin, and the magnetic field direction. Each of these bases are orthonormal within their species blocks. It is also to be recognized that they are to be taken as orthogonal between blocks.

Finally, for the breakup reaction  $\text{MuX} \cdot^* \rightarrow \text{Mu} + X$ , the gas molecule  $X$  that is liberated may carry away whichever tensorial component of the rotational angular momentum of the metastable radical was present at the time of reaction. Thus a basis element for this molecule is required even though it is lost to the background gas. The basis elements

$$\Phi_n^X = \frac{1}{\sqrt{2n+1}} \mathcal{Y}^{(n)}(\mathbf{J}) \odot^n \mathcal{Y}^{(n)}(\hat{\mathbf{B}}) \quad (42)$$

are orthonormal with respect to each other. On the other hand, when the formation reaction occurs, only the scalar or  $n=0$  component will be allowed since the background gas is assumed to be in rotational equilibrium, specifically having no directional preference for its rotational motion.

Matrix elements of the motion generator (38) in this basis are required to numerically solve for the complex eigenval-

ues and eigenvectors, which can then be related to the observed signals. Free-motion Liouville spin dynamical matrix elements have been discussed in Refs. [19,20], as have the collisional reorientation matrix elements. The former are quite involved, while the latter are assumed to be diagonal, whose diagonal elements are the reciprocals of the corresponding reorientation collision lifetimes. These lifetimes depend on the rotational ( $\mathbf{J}$ ) angular momentum index  $n$ , being finite if  $n$  is nonzero and infinite for  $n$  equal to zero. As stated earlier, the rationale for this parametrization is the assumption that the electron and muon spins play a negligible role in the collision process, so they should neither be affected by nor influence what happens to the molecules orientation. Since the rates are inversely proportional to the lifetimes, there is no relaxation for the scalar component of the angular momentum tensorial behavior. The lifetimes are also inversely proportional to the "total" number density of the gas since it is assumed that all collision partners are equally efficient at causing reorientation or, equivalently, that the difference between reorientation collisions of the molecular radicals with the different gas molecules  $X$  and  $Y$  may be ignored.

Both the metastable and stable molecular radicals can be described using similar basis elements [19,20]. The metastable basis is a function of the three spin vectors  $\mathbf{I}$ ,  $\mathbf{S}$ ,  $\mathbf{J}$ , and the field direction  $\hat{\mathbf{B}}$ , that is,

There are six different chemical reaction rate superoperators to consider, the first two being the loss and gain terms for the muonium radical. The loss term  $\mathcal{R}_{\text{Mu}}$  represents the loss of muonium due to the forward (addition) reaction that produces the metastable radical  $\text{MuX} \cdot^*$  and the exchange reaction producing the stable radical  $\text{MuX} \cdot$ . Furthermore, the reactant gas molecules are assumed to be in thermal equilibrium so that only the  $n=0$  rotational angular momentum term for the reactant  $X$  molecule will contribute. This chemical reaction rate superoperator is in the  $5 \times 5$  muonium block of the full motion generator matrix. Specifically, the matrix elements for the loss of muonium are assumed to be of the form

$$\langle\langle \Phi_N | \mathcal{R}_{\text{Mu}} | \Phi_{N'} \rangle\rangle = \lambda_{\text{Mu}}^L \delta_{NN'}, \quad 1 \leq N \leq 5, \quad (43)$$

where  $\lambda_{\text{Mu}}^L$  is given by Eq. (31). This loss term is diagonal in the muonium block since the collisions causing chemical reaction are assumed to have no direct affect upon the spins of the muonium radical as it adds to molecule  $X$  or reacts with the complex  $XY$ .

The second is the gain term for the muonium radical. This term  $\mathcal{P}_{\text{Mu}, \text{MuX} \cdot^*}$  represents the gain of muonium from the breakup of the metastable radical  $\text{MuX} \cdot^*$  in a unimolecular



process. This chemical reaction rate superoperator lies in the off-diagonal block of the motion generator that couples the metastable radical to the muonium radical. In the breakup reaction it is assumed that the liberated gas molecule  $X$  may carry off the tensorial component of the rotational angular momentum of the metastable radical. Since this gas molecule becomes one of the molecules in the bulk gas, this nonequilibrium angular momentum is lost and will thus play no further role in the spin dynamics. On the assumption that the muon and electron spins have no effect on the collision process, it follows that the matrix elements of this superoperator in the longitudinal bases reduce to the overlap of the combined basis for the muonium and the molecule  $X$ , with the metastable molecular radical, that is,

$$\begin{aligned} & \langle\langle \Phi_N | \text{Tr}_X^{\text{int}} \Phi_n^X [ \mathcal{P}_{\text{Mu}, \text{Mu}X^*} ] | \Phi_{N'} \rangle\rangle \\ &= \lambda_{\text{Mu}}^G \langle\langle \Phi_n^X \Phi_N | \Phi_{N'} \rangle\rangle \\ &= \lambda_{\text{Mu}}^G \delta_{mm'} \delta_{nn'} \delta_{pp'} \sqrt{(2\alpha' + 1)(2r + 1)(2r' + 1)} \\ & \quad \times (-1)^{p + \alpha' + r'} (-1)^{(r + r' + n)/2} \begin{pmatrix} r & r' & n \\ 0 & 0 & 0 \end{pmatrix} \\ & \quad \times \begin{Bmatrix} m & p & r \\ r' & n & \alpha' \end{Bmatrix}, \end{aligned} \quad (44)$$

where  $1 \leq N \leq 5$  and  $6 \leq N' \leq 40$ ,  $()$  and  $\{ \}$  are the standard  $3-j$  and  $6-j$  symbols [33], and  $\lambda_{\text{Mu}}^G$  is given by Eq. (31). Again, since the chemical reactions are assumed to be independent of the spins of the muon and electron, the tensorial nature of these spins is the same for both reactant and product radicals.

The third and fourth chemical reaction rate superoperators are the loss and gain terms for the metastable molecular radical. The loss term  $\mathcal{R}_{\text{Mu}X^*}$  represents the loss of the metastable radical due to the decomposition reaction, which produces muonium, and due to the stabilization reaction, which results in the stable radical  $\text{Mu}X\cdot$ . Collisions with either molecular gas species  $X$  or  $Y$  may contribute to both these processes. This chemical reaction rate superoperator lies in the  $35 \times 35$  metastable radical diagonal block of the full motion generator matrix with its matrix elements assumed to be of the form

$$\langle\langle \Phi_N | \mathcal{R}_{\text{Mu}X^*} | \Phi_{N'} \rangle\rangle = \lambda_{\text{Mu}X^*}^L \delta_{NN'}, \quad (45)$$

for  $N$  between 6 and 40 and  $\lambda_{\text{Mu}X^*}^L$  is given by Eq. (31). This loss term is diagonal in the metastable radical block since the chemical reactions are assumed to have no direct affect upon the spins of the electron and the muon. For the rotational angular momentum, it is assumed that the gas molecule  $X$  carries off the appropriate tensorial component in the decomposition reaction, while for the stabilization reaction, all the stable radical's angular momentum tensorial form will be the same as the metastable's. The fourth reaction is the gain term for the metastable radical. This term  $\mathcal{P}_{\text{Mu}X^*, \text{Mu}}$  represents the gain of the metastable radical from the formation reaction between muonium and a reactive gas molecule  $X$ . As before, the reactant gas molecules are assumed to be in thermal equilibrium so that only the  $n=0$  rotational angular momentum

term for the reactant  $X$  molecule will contribute and thus only the scalar tensorial component of the metastable radical will be formed. This chemical reaction rate superoperator lies in the off-diagonal block of the motion generator that couples the muonium radical to the metastable radical. Matrix elements of this superoperator in the longitudinal bases are explicitly

$$\langle\langle \Phi_N | \mathcal{P}_{\text{Mu}X^*, \text{Mu}} | \Phi_{N'} \rangle\rangle = \lambda_{\text{Mu}X^*}^G \delta_{mm'} \delta_{n0} \delta_{pp'} \delta_{rr'} \delta_{\alpha m}, \quad (46)$$

where  $6 \leq N \leq 40$  and  $1 \leq N' \leq 5$ . Again the chemical reactions are assumed to be independent of the spins of the muon and electron so that the tensorial nature of these spins is the same for both radicals. The production of the stable radical by the third-order reaction (28) is assumed to have the same form

$$\langle\langle \Phi_N | \mathcal{P}_{\text{Mu}X, \text{Mu}} | \Phi_{N'} \rangle\rangle = \lambda_T \delta_{mm'} \delta_{n0} \delta_{pp'} \delta_{rr'} \delta_{\alpha m}, \quad (47)$$

where  $41 \leq N \leq 75$  and  $1 \leq N' \leq 5$ .

The final collisional term is the gain of the stable molecular radical by stabilization of the unstable radical. Note that there is no loss term  $\mathcal{R}_{\text{Mu}X}$  for chemical reactions since this radical is stable. However, as stated above, there will be reorientation loss terms for this radical. The gain term for the stable molecular radical  $\mathcal{P}_{\text{Mu}X, \text{Mu}X^*}$  represents the gain of the stable molecular radical from the stabilization reaction during a collision between either molecular gas  $X$  or  $Y$  and the metastable radical  $\text{Mu}X^*$ . The chemical reaction rate for this process  $k_s$  is assumed to be the same for reactions of  $\text{Mu}X^*$  with either  $X$  or  $Y$ . This chemical reaction rate superoperator lies in the off-diagonal block of the motion generator that couples the stable radical to the metastable radical. Explicitly, matrix elements of this superoperator in the longitudinal basis are

$$\begin{aligned} \langle\langle \Phi_N | \mathcal{P}_{\text{Mu}X, \text{Mu}X^*} | \Phi_{N'} \rangle\rangle &= \lambda_S \delta_{mm'} \delta_{nn'} \delta_{pp'} \delta_{rr'} \delta_{\alpha' \alpha} \\ &= \lambda_S \delta_{N(N'+35)}, \end{aligned} \quad (48)$$

where  $41 \leq N \leq 75$  and  $6 \leq N' \leq 40$ . Again the chemical reactions are assumed to be independent of the spins of the muon and electron so that the tensorial nature of these spins is the same for both reacting radicals. For the rotational angular momentum, it is assumed that the stable radical's angular momentum tensorial component is the same as the metastable's in the stabilization reaction.

## B. Transverse basis

For  $C_{\infty v}$  symmetry, a right-handed (complex) three-dimensional coordinate system may be constructed from the magnetic field direction  $\hat{\mathbf{B}} = \hat{\mathbf{z}}$ , the positively rotating unit vector  $\hat{\mathbf{e}}_+ = (\hat{\mathbf{x}} + i\hat{\mathbf{y}})/\sqrt{2}$ , and the negatively rotating unit vector  $\hat{\mathbf{e}}_- = (\hat{\mathbf{x}} - i\hat{\mathbf{y}})/\sqrt{2}$ . The positively rotating unit vector can be used to construct the transverse basis  $\Psi_N$  [19,20]. In the present system, this basis has 64 elements: 4 for muonium, 30 for the metastable radical, and 30 for the stable radical. As with the longitudinal basis, both the metastable and stable molecular radicals can be described using similar basis ele-

ments [20]. The metastable basis will be a function of the three spin vectors  $\mathbf{I}$ ,  $\mathbf{S}$ , and  $\mathbf{J}$  and the positively rotating vector  $\hat{\mathbf{e}}_+$ , that is,

$$\Psi_N = (2r+3) \sqrt{\frac{2(2\alpha+1)}{r+2}} \mathcal{Y}^{(n)}(\mathbf{J}) \mathcal{Y}^{(m)}(\mathbf{S}) \odot^{m+n} \mathbf{V}(m, n, \alpha) \odot^\alpha \mathbf{V}(\alpha, p, r+1) \odot^{r+1} \mathbf{V}(r+1, 1, r) \odot^{r+1+p} \mathcal{Y}^{(r)}(\hat{\mathbf{B}}) \hat{\mathbf{e}}_+ \mathcal{Y}^{(p)}(\mathbf{I}),$$

$$5 \leq N \leq 34. \quad (49)$$

The stable radical basis elements have the same form, but the numbering is  $35 \leq N \leq 64$ . Again the numerical index  $N$  for the molecular radicals is used to classify the set of parameters  $mnpr\alpha$  [20]. For the muonium elements ( $1 \leq N \leq 4$ ), the basis requires the coupling of the electron's spin  $\mathbf{S}$ , the muon's spin  $\mathbf{I}$ , and the positively rotating vector  $\hat{\mathbf{e}}_+$ ,

$$\Psi_N = (2r+3) \sqrt{\frac{2}{r+2}} \mathcal{Y}^{(m)}(\mathbf{S}) \odot^m \mathbf{V}(m, p, r+1) \odot^{r+1} \mathbf{V}(r+1, 1, r) \odot^{r+1+p} \mathcal{Y}^{(r)}(\hat{\mathbf{B}}) \hat{\mathbf{e}}_+ \mathcal{Y}^{(p)}(\mathbf{I}), \quad 1 \leq N \leq 4. \quad (50)$$

This four-dimensional part of the transverse basis is orthonormal and is a special case of Eq. (49). The indexing scheme  $N$  for this portion of the basis involves  $m$ ,  $p$ , and  $r$ , the tensorial orders of the spins and the magnetic field. For the decomposition reaction from  $\text{MuX}^*$  to  $\text{Mu}$  and  $X$ , the gas molecule  $X$  that is liberated may carry away whatever tensorial component of the rotational angular momentum of the metastable radical was present at the time of reaction. It is also possible for either the muonium or  $X$  to carry off the rotating  $\hat{\mathbf{e}}_+$  tensorial component. If the muonium carries off the rotating tensorial component, the above muonium basis will be coupled to the gas molecule (longitudinal) basis

$$\Phi_n^X = \frac{1}{\sqrt{2n+1}} \mathcal{Y}^{(n)}(\mathbf{J}) \odot^n \mathcal{Y}^{(n)}(\hat{\mathbf{B}}). \quad (51)$$

However, when the  $X$  molecule carries off the rotating tensorial component, the two bases are, for muonium and  $X$ , respectively,

$$\Phi_M = \mathcal{Y}^{(m)}(\mathbf{S}) \odot^m \mathbf{V}(m, p, r) \odot^{r+p} \mathcal{Y}^{(r)}(\hat{\mathbf{B}}) \mathcal{Y}^{(p)}(\mathbf{I}), \quad (52)$$

$$\Psi_q^X = \sqrt{\frac{2(2q+3)}{q+2}}$$

$$\times \mathcal{Y}^{(q+1)}(\mathbf{J}) \odot^{q+1} \mathbf{V}(q+1, 1, q) \odot^{q+1} \mathcal{Y}^{(q)}(\hat{\mathbf{B}}) \hat{\mathbf{e}}_+,$$

where the subscripts distinguish these bases from the previous bases. Each species block of this basis set is orthonormal within itself and required to be orthonormal between the species blocks.

As with the longitudinal field, there are six different chemical reaction superoperators to consider. The chemical and spin arguments for the behaviors of these transverse basis matrix elements are the same as for the longitudinal situation. For the first reaction superoperator, the matrix elements for the loss term  $\mathcal{R}_{\text{Mu}}$  lies in the  $4 \times 4$  muonium diagonal block of the motion generator matrix

$$\langle \langle \Psi_N | \mathcal{R}_{\text{Mu}} | \Psi_{N'} \rangle \rangle = \lambda_{\text{Mu}}^L \delta_{NN'}, \quad 1 \leq N \leq 4. \quad (53)$$

This loss term is diagonal in the muonium block and is due to the addition chemical reactions. The second reaction su-

peroperator is the gain term for the muonium radical  $\mathcal{P}_{\text{Mu}, \text{MuX}^*}$  because of the decomposition reaction. There are two contributions to this gain term, depending upon whether the muonium or the liberated gas molecule carries off the rotating tensorial component. This chemical reaction rate matrix lies in the off-diagonal block of the motion generator that couples the metastable radical to the muonium radical. When the muonium carries off the rotational tensorial component, this reaction matrix becomes

$$\begin{aligned} & \langle \langle \Psi_N | T_{\text{X}}^{\text{int}} \Phi_n^X [ \mathcal{P}_{\text{Mu}, \text{MuX}^*} ] | \Psi_{N'} \rangle \rangle \\ &= \lambda_{\text{Mu}}^G \langle \langle \Phi_n^X \Psi_N | \Psi_{N'} \rangle \rangle \\ &= \lambda_{\text{Mu}}^G \delta_{mm'} \delta_{nn'} \delta_{pp'} (-1)^{p+r'+\alpha'+1} \\ & \quad \times \left[ \frac{(2r+3)(2r'+3)\sqrt{2\alpha'+1}}{\sqrt{(2n+1)(r+2)(r'+2)}} \right] \\ & \quad \times \begin{Bmatrix} n & r+1 & r'+1 \\ p & \alpha' & m \end{Bmatrix} T_{nr'r}, \end{aligned} \quad (54)$$

where  $1 \leq N \leq 4$ ,  $5 \leq N' \leq 34$ , and the coupling coefficient is

$$\begin{aligned} T_{abc} &= (-1)^{(a+b+c)/2} \sqrt{(2a+1)(2b+1)(2c+1)} \\ & \quad \times \begin{pmatrix} a & b & c \\ 0 & 0 & 0 \end{pmatrix} \begin{Bmatrix} a & b+1 & c+1 \\ 1 & c & b \end{Bmatrix} \\ & \quad + (-1)^{(a+b+c)/2} \sqrt{\frac{(2a+1)(b+1)(c+1)}{(2b+3)(2c+3)}} \\ & \quad \times \begin{pmatrix} a & b+1 & c+1 \\ 0 & 0 & 0 \end{pmatrix} - i \sum_l (-1)^{l+(a+b+c+1)/2} \\ & \quad \times (2l+1) \sqrt{6(2a+1)(2b+1)(2c+1)} \begin{pmatrix} b & c & l \\ 0 & 0 & 0 \end{pmatrix} \\ & \quad \times \begin{pmatrix} a & l & 1 \\ 0 & 0 & 0 \end{pmatrix} \begin{Bmatrix} a & b+1 & c+1 \\ l & b & c \\ 1 & 1 & 1 \end{Bmatrix}. \end{aligned} \quad (55)$$

The last set of curly brackets in this equation is a standard 9- $j$  symbol [33]. On the other hand, when the gas molecule carries off the rotational tensorial component, this reaction matrix becomes

$$\begin{aligned} \langle\langle \Phi_M | \text{Tr}_X^{\text{int}} \Psi_q^X [\mathcal{P}_{\text{Mu}, \text{MuX}^*}] | \Psi_{N'} \rangle\rangle &= \lambda_{\text{Mu}}^G \langle\langle \Psi_q^X \Phi_M | \Psi_{N'} \rangle\rangle \\ &= \lambda_{\text{Mu}}^G \delta_{mm'} \delta_{n'(q+1)} \delta_{pp'} (-1)^{p+q+r+\alpha'+1} 2(2r'+3) \\ &\quad \times \sqrt{\frac{(2\alpha'+1)(2q+3)}{(q+2)(r'+2)}} \left\{ \begin{matrix} r & q+1 & r'+1 \\ \alpha' & p & m \end{matrix} \right\} T_{rqr'}, \end{aligned} \quad (56)$$

where  $1 \leq M \leq 4$  and  $5 \leq N' \leq 34$ . The total contribution from this gain rate is a weighted sum of the two separate terms wherein the weights  $g_{\text{Mu}}$  and  $g_X$  ( $g_{\text{Mu}} + g_X = 1$ ) are taken to be fitting parameters. These rate matrices are due to the reverse (decomposition) chemical reaction.

The third and fourth chemical reaction matrices are due to the loss and gain terms for the metastable molecular radical. The loss term  $\mathcal{R}_{\text{MuX}^*}$  represents the loss of the metastable radical and lies in the  $30 \times 30$  metastable radical diagonal block of the motion generator matrix

$$\langle\langle \Psi_N | \mathcal{R}_{\text{MuX}^*} | \Psi_{N'} \rangle\rangle = \lambda_{\text{MuX}^*}^L \delta_{NN'} \quad (57)$$

for  $N$  and  $N'$  between 5 and 34. This loss term is diagonal in the metastable radical block and involves the loss of the metastable radical, both to muonium by  $\lambda_R$  and to the stable radical by  $\lambda_S$ . The fourth reaction matrix is for the gain of the metastable radical  $\mathcal{P}_{\text{MuX}^*, \text{Mu}}$ . This chemical reaction rate matrix lies in the off-diagonal block of the motion generator that couples the muonium radical to the metastable radical

$$\langle\langle \Psi_N | \mathcal{P}_{\text{MuX}^*, \text{Mu}} | \Psi_{N'} \rangle\rangle = \lambda_{\text{MuX}^*, \text{Mu}}^G \delta_{mm'} \delta_{n0} \delta_{pp'} \delta_{rr'} \delta_{\alpha m}, \quad (58)$$

where  $5 \leq N \leq 34$  and  $1 \leq N' \leq 4$ . The third-order production of the stable radical is analogous,

$$\langle\langle \Psi_N | \mathcal{P}_{\text{MuX}, \text{Mu}} | \Psi_{N'} \rangle\rangle = \lambda_T \delta_{mm'} \delta_{n0} \delta_{pp'} \delta_{rr'} \delta_{\alpha m}, \quad (59)$$

where  $35 \leq N \leq 64$  and  $1 \leq N' \leq 4$ . The final reaction is the gain of the stable molecular radical by stabilization  $\mathcal{P}_{\text{MuX}, \text{MuX}^*}$ . The chemical reaction rate for this process is  $\lambda_S$ , while this chemical reaction rate matrix lies in the off-diagonal block of the motion generator that couples the stable radical to the metastable radical

$$\begin{aligned} \langle\langle \Psi_N | \mathcal{P}_{\text{MuX}, \text{MuX}^*} | \Psi_{N'} \rangle\rangle &= \lambda_S \delta_{mm'} \delta_{nn'} \delta_{pp'} \delta_{rr'} \delta_{\alpha \alpha'} \\ &= \lambda_S \delta_{N(N'+30)}, \end{aligned} \quad (60)$$

where  $35 \leq N \leq 64$  and  $5 \leq N' \leq 34$ .

#### IV. OBSERVED SIGNALS

The experiments [5,6,13,27] are carried out in either the longitudinal or the transverse configuration. An identification of what formal quantity corresponds to what type of signal that is measured in the  $\text{C}_2\text{H}_4\text{Mu}\cdot$  problem was presented in Ref. [20]. This result must be extended to include the different chemical species that are present since all species can

contribute to the signals and thus need, in general, to be included. As depicted in the Introduction, the observable signal is the sum of the contributions from each chemical species. These contributions cannot be individually identified in the experiments.

#### A. Longitudinal signals

The experiments carried out in longitudinal field detect the component of the muon spin in the magnetic field direction. There will be a diamagnetic fraction  $f_D$  at the zero of count time that plays no role in the chemical dynamics and a fraction that plays a role in the chemical dynamics. Thus the signal can be expressed in terms of the longitudinal basis [20] using

$$\begin{aligned} S^L(t) &= \hat{\mathbf{B}} \cdot \langle \mathbf{I} \rangle (t) = \text{Tr}_r \hat{\mathbf{B}} \cdot \mathbf{I} \rho(t) \\ &= \frac{1}{2} \langle\langle \Phi_1 + \Phi_6 + \Phi_{41} | \rho(t) \rangle\rangle + f_D \langle I_B \rangle, \end{aligned} \quad (61)$$

where  $\Phi_1$ ,  $\Phi_6$ , and  $\Phi_{41}$  are the elements of the longitudinal basis that represent the longitudinal component of the muon's spin angular momentum in each of the radicals present in the chemically reacting system. The time dependence, which is governed by  $\mathcal{G}$ , can be expressed in terms of its eigenvalues  $\lambda_j^L$  and eigenfunctions

$$\varphi_j = \sum_{N=1}^{75} \Phi_N c_{jN} \quad (62)$$

in the longitudinal basis, namely,

$$\begin{aligned} \rho(t) &= e^{-\mathcal{G}t} \rho(0) = \sum_{j=1}^{75} e^{-\mathcal{G}t} \varphi_j p_j(0) \\ &= \sum_{j=1}^{75} \varphi_j e^{-\lambda_j^L t} p_j^L(0). \end{aligned} \quad (63)$$

The observed signal (61) is thus a sum of complex exponentials and amplitudes

$$\begin{aligned} S^L(t) &= A_0 + \sum_{j=1}^{75} e^{-\lambda_j^L t} p_j^L(0) \langle\langle \Phi_1 + \Phi_6 + \Phi_{41} | \varphi_j \rangle\rangle \\ &= A_0 + \sum_{j=1}^{75} e^{-\lambda_j^L t} p_j^L(0) [c_{j1}^L + c_{j6}^L + c_{j41}^L] \\ &= A_0 + \sum_{j=1}^{75} e^{-\lambda_j^L t} A_j^L, \end{aligned} \quad (64)$$

where  $A_0 = \frac{1}{2} f_D$ . For the experiments involving  $\text{C}_2\text{H}_4\text{Mu}\cdot$  at high partial pressure, the muon slowed down, formed muonium, and reacted with ethene to form a stable radical, all before counting began. To fit the data, it was sufficient [20] to assume that at the zero of count time, only the muon spin was out of equilibrium and that this spin was pointed in the  $\hat{\mathbf{B}}$  direction. However, for a system such as the reaction with CO, where the muon slows down, forms muonium, and then reacts with the gas after counting begins, the proper initial state to be used in the theoretical calculation becomes ques-

tionable. Specifically, there is the question as to whether there is some probability that the muon needs to be treated as if it is attached to the molecular fragment at the initial count time. The present treatment allows a fraction  $f_{\text{Mu}}$  of the muon spins to be in muonium and a fraction  $f_{\text{MuX}^*}$  where the muon spin is attached to the molecule. (There is also the fraction  $f_D$  that is diamagnetic at the zero of the count time and plays no role in the subsequent precession-relaxation dynamics.) Formally this is the requirement that the initial muon spin expectation value  $\langle \mathbf{I} \rangle = \hat{\mathbf{B}}/2$  is to be interpreted in the nonequilibrium part of the spin density operator as

$$\rho^{\text{ne}}(0) = \frac{1}{2}f_{\text{Mu}}\Phi_1 + \frac{1}{2}f_{\text{MuX}^*}\Phi_6 = \sum_{j=1}^{75} \varphi_j^L p_j^L(0). \quad (65)$$

This sum over the eigenvectors needs to be inverted in order to identify the expansion coefficients  $p_j^L(0)$ . Since the motion generator  $\mathcal{G}$  is not Hermitian or even necessarily normal, the eigenvectors are not necessarily orthogonal. Thus the inversion requires the use of the eigenvector overlap matrix

$$\mathcal{O}_{jk}^L \equiv \langle \langle \varphi_j^L | \varphi_k^L \rangle \rangle = \sum_{N=1}^{75} c_{jN}^{L*} c_{kN}^L. \quad (66)$$

In this way, the expansion coefficients  $p_j^L(0)$  are calculated to be

$$\begin{aligned} p_j^L(0) &= \sum_{k=1}^{75} [(\mathcal{O}^L)^{-1}]_{jk} \langle \langle \varphi_k^L | \rho^{\text{ne}}(0) \rangle \rangle \\ &= \frac{1}{2} \sum_{k=1}^{75} [(\mathcal{O}^L)^{-1}]_{jk} [f_{\text{Mu}} c_{k1}^{L*} + f_{\text{MuX}^*} c_{k6}^{L*}], \end{aligned} \quad (67)$$

while the amplitude of the signal in the  $j$ th eigenmode of  $\mathcal{G}$  is

$$\begin{aligned} A_j^L &= \frac{1}{2} \sum_{k=1}^{75} [c_{j1}^L + c_{j6}^L + c_{j41}^L] [(\mathcal{O}^L)^{-1}]_{jk} \\ &\quad \times [f_{\text{Mu}} c_{k1}^{L*} + f_{\text{MuX}^*} c_{k6}^{L*}]. \end{aligned} \quad (68)$$

The complex eigenvalues  $\lambda_j^L = \eta_j^L + i\omega_j^L$  may be expressed in terms of relaxation rates  $\eta_j^L$  and frequencies  $\omega_j^L$ . For the longitudinal setup, some of the frequencies will be zero and the signal can be expressed as the sum of contributions from eigenvalues of zero and nonzero frequency

$$\begin{aligned} S^L(t) &= A_0 + \sum_{j \ni \omega_j^L = 0} e^{-\eta_j^L t} A_j^L \\ &\quad + \sum_{j \ni \omega_j^L \neq 0} e^{-\eta_j^L t} \cos(\omega_j^L t + \theta_j^L) |A_j^L| \end{aligned} \quad (69)$$

since for each term with frequency  $\omega_j^L$  there is a corresponding term with frequency  $-\omega_j^L$  and complex conjugate amplitude. Thus for each mode a relaxation rate and an amplitude may, in principle, be measured. In carrying out the experiments, the nonzero frequencies are found to be too large to be measured, so that the signal is then simply given by the zero-frequency components

$$S^L(t) = A_0 + \sum_{j \ni \omega_j^L = 0} e^{-\eta_j^L t} A_j^L. \quad (70)$$

Since, in general, there may be a number of modes that contribute to the observed signal, fitting problems can arise. For example, it is not possible to distinguish the chemical environment that the muon is in, that is, it may be in any of the species present in the gas. Thus all three radicals need to be included in the theoretical description of the longitudinal signal. In addition, there may be some fields and pressures where only a single mode is populated and others where two or more modes contribute. Care must be taken both in carrying out the experiments and in their theoretical interpretation to ensure that these various situations are treated properly.

## B. Transverse signals

The experiments carried out in transverse field detect the component of the muon spin that rotates in the plane perpendicular to the magnetic field direction. Here this is analyzed according to the positively rotating component of the spin, that is,

$$\begin{aligned} S^+(t) &= \hat{\mathbf{e}}_+ \cdot \langle \mathbf{I} \rangle(t) \\ &= f_D \hat{\mathbf{e}}_+ \cdot \langle \mathbf{I} \rangle(t) + \frac{1}{2} \langle \langle \Psi_1 + \Psi_5 + \Psi_{35} | \rho(t) \rangle \rangle. \end{aligned} \quad (71)$$

As with the longitudinal signal, this transverse result may be expressed as

$$S^+(t) = \frac{1}{2} f_D e^{-i\omega_\mu t} + \sum_{j=1}^{64} e^{-\lambda_j^T t} A_j^T, \quad (72)$$

where the amplitudes are the transverse analogs of the longitudinal amplitudes, specifically

$$\begin{aligned} A_j^T &= \frac{1}{2} \sum_{k=1}^{64} [c_{j1}^T + c_{j5}^T + c_{j35}^T] [(\mathcal{O}^T)^{-1}]_{jk} \\ &\quad \times [f_{\text{Mu}} c_{k1}^{T*} + f_{\text{MuX}^*} c_{k5}^{T*}], \end{aligned} \quad (73)$$

under the same assumptions about the initial nonequilibrium part at the zero of the count time. The complex eigenvalues  $\lambda_j^T = \eta_j^T + i\omega_j^T$  may also be expressed in terms of relaxation rates  $\eta_j^T$  and frequencies  $\omega_j^T$ . For the (real-valued) transverse signal, none of these have zero frequency, so that the real part of the signal becomes a series of damped cosines

$$\begin{aligned} S^T(t) &= \text{Re} S^+(t) = \frac{1}{2} f_D \cos(\omega_\mu t) \\ &\quad + \sum_{j=1}^{64} e^{-\eta_j^T t} \cos(\omega_j^T t + \theta_j^T) |A_j^T|. \end{aligned} \quad (74)$$

Thus for each mode there are four observable quantities: the relaxation rate, the frequency, the phase angle, and the amplitude. As opposed to longitudinal fields, the additional experimental information of the different observed frequencies

TABLE I. Preliminary global fitting parameters.

Parameter	Value	Error
$\omega_0$ (rad/ $\mu$ s)	3830.0	800.0
$\omega_{SR}$ (rad/ $\mu$ s)	-85.0	11.0
$\omega_{IR}$ (rad/ $\mu$ s)	-37.0	10.0
$\gamma_J$ (rad/ $\mu$ s G)	0.070	0.25
$k_1$ (cm <sup>3</sup> /s)	$3.39 \times 10^{-13}$	$1.08 \times 10^{-13}$
$k_{fb}$ (cm <sup>3</sup> /s)	$1.74 \times 10^{-11}$	$0.83 \times 10^{-11}$
$k_{ft}$ (cm <sup>6</sup> /s)	$35.3 \times 10^{-34}$	$10.1 \times 10^{-34}$
$k_r$ (1/s)	$1.61 \times 10^9$	$0.54 \times 10^9$
$k_s$ (cm <sup>3</sup> /s)	$7.87 \times 10^{-16}$	$8.69 \times 10^{-16}$

can be of immense help in the fitting procedure, provided, of course, the amplitudes are nonzero.

## V. DISCUSSION

The theoretical description of the signals associated with the muon spin relaxation of muonated gaseous radicals has been extended to include situations where the radicals are formed in slow processes as opposed to fast processes. For fast processes (due to a high enough partial pressure of the reacting gas) the muonated radicals are formed before data collection begins and are stable and their observed dynamical modes are relaxed through reorientation collisions. On the other hand, for slow processes (at low partial pressures of the reacting gases) where the radicals are formed during the period of time when data are being collected, the chemical reactions play a role in determining the precession-relaxation modes of the muon system, as do the reorientation collisions. In the current approach, it is assumed that there are three different radicals that are important, specifically, the muonium radical and both unstable  $\text{MuX}^{\bullet}$  and stable  $\text{MuX}$ -molecular addition radicals. As a consequence, there are 22 possible parameters to be fit to the experimental data under the full theory, which consist of the following: For each molecular radical, there are five frequencies  $\omega_0, \omega_J = \gamma_J B, \omega_{SR}, \omega_{IR}$ , and  $c_A$  that characterize the spin Hamiltonian [see Eq. (25)] and two reorientational relaxation times  $\tau_1$  and  $\tau_2$  for a total of 14 parameters associated with the motions of the two radicals. The chemical dynamics intro-

duces 4 reaction rate constants  $k_{fb}$ ,  $k_{ft}$ ,  $k_r$ , and  $k_s$  and 2 breakup fractions  $g_{\text{Mu}}$  and  $g_X$  in transverse fields. Finally, there are 2 initial fractions  $f_{\text{Mu}}$  and  $f_{\text{MuX}^{\bullet}}$ . To determine all these parameters unambiguously requires a large amount of accurate data in both the longitudinal and transverse configurations.

Experiments have been performed and are currently being performed with the diamagnetic reactant gas carbon monoxide with and without argon and nitrogen as dopant gases [5,6,27]. The fitting and analysis of the raw data are in the preliminary phase [6,27]. At present, preliminary fits of this raw data to Eqs. (2) and (3) have been performed under the assumption of single exponential relaxation modes. Since the target gases are all diamagnetic, no spin exchange processes occur and only the indirect effects of the chemical reactions and the reorientation collisions of the molecular radicals cause the muon spins to relax. In longitudinal fields, the assumed, and fitted, single zero-frequency relaxation mode has a rate that varies with the field and pressure. In general, this rate decreases with increasing field. As relaxation of the muon spin does occur, there must be a mode of decay of the molecular radical since, if there were only forward reactions, then no relaxation of the muon spin would be observed; see Eqs. (11) and (17). This decay can be associated with a reverse chemical reaction [5,6] as well as spin reorientation and the stabilization of the molecular radical. In transverse fields only the two modes having the lowest frequencies that are close to those associated with muonium have been observed [5,6,27] and no precession-relaxation modes have been observed with frequencies that are close to the  $\text{MuCO}$  radical frequencies. This suggests that the observed modes of relaxation have a large muonium component and that the decay rate of the molecular radical dominates the forward rate to such an extent that the metastable radical does not have an appreciable lifetime on the minimum time step of the experiments, which is a few nanoseconds. For intermediate fields where the two modes are resolvable, the relaxation rates agree within experimental uncertainty, while for lower fields, where the frequency difference is not resolvable, only a single exponential decay rate has been used to fit the experimental data.

Preliminary fittings, both of the raw data to Eqs. (2) and (3) assuming single exponentials and of the resulting relax-

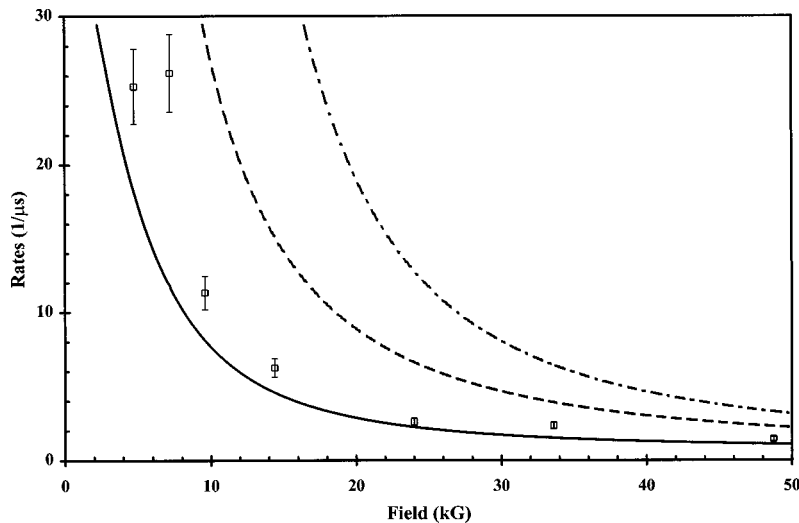


FIG. 1. Experimental longitudinal muon spin relaxation rate versus magnetic field in 40.0 atm of pure CO. The solid curve is the global fit, while the squares are the experimental points with estimated errors. The dashed line is the next lowest relaxation rate with appreciable amplitude, while the dash-dotted line is the third lowest rate.

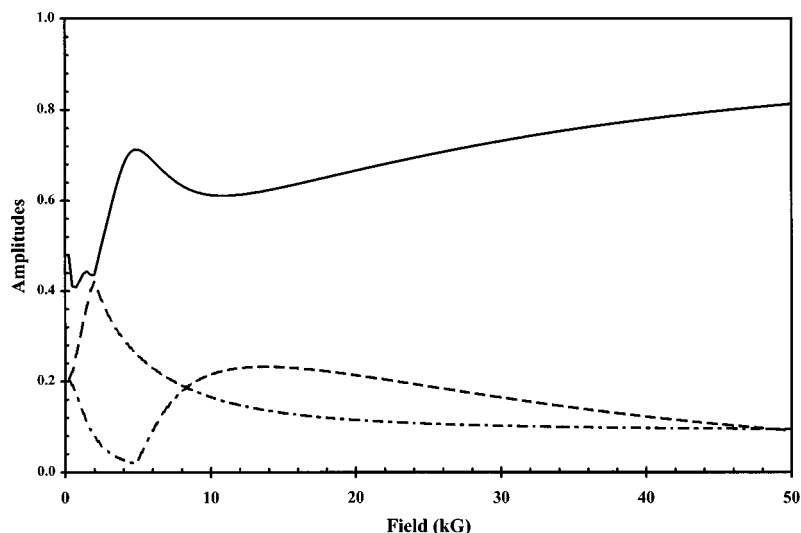


FIG. 2. Predicted longitudinal amplitudes. The solid curve is the amplitude of the lowest mode, the dashed line is the amplitude of the next lowest mode, and the dash-dotted line is the amplitude of the third lowest mode.

ation rates to the theory presented in this paper, indicate that the present theory appears to be sufficient to fit the experimental data. For the preliminary theoretical fit, the parameter set has been reduced to nine parameters since the inclusion of more parameters does not improve the fit and also results in very large uncertainties in the parameters. With this limitation in mind, the fitting was carried out by combining the components of the density operator associated with the metastable and stable radicals. This approximation cuts down the size of the matrices and assumes that the Hamiltonian parameters of these species are essentially equal. Since the metastable and stable radicals are not distinguished in this approximation, the gain and loss rates for the chemical species Mu and Ra (composite of metastable and stable radicals) have been adjusted to mimic the chemical kinetics as

$$\begin{aligned} \lambda_{\text{Mu}}^L &= \lambda_F + \lambda_T, & \lambda_{\text{Mu}}^G &= R\lambda_R, \\ \lambda_{\text{Ra}}^G &= \lambda_F + \lambda_T, & \lambda_{\text{Ra}}^L &= R[\lambda_R + \lambda_S], \end{aligned} \quad (75)$$

where the parameter  $R$  is the ratio of the formation rate of the metastable radical to the sum of the formation rates of both radicals,

$$R = \frac{k_{fb}}{k_{fb} + k_{ft}n_Y}. \quad (76)$$

This takes into account the fraction of the molecular radical that is metastable. It was further discovered that the inclusion of the dipolar coupling constant  $c_A$  did not improve the fit, so its presence was ignored by setting  $c_A$  equal to zero.

The fit was now carried out allowing variation of the four frequencies  $\omega_0$ ,  $\omega_{SR}$ ,  $\omega_{IR}$ , and  $\omega_J = \gamma_J B$ , one reorientation rate  $k_1 = 1/\tau_1$ , and the four chemical rates  $k_{fb}$ ,  $k_{ft}$ ,  $k_r$ , and  $k_s$ . With this limited set, a preliminary simultaneous global fit to both the longitudinal and transverse data was accomplished with the parametric results given in Table I. Representative longitudinal and transverse results are given in Figs. 1 and 2 and Figs. 3 and 4, respectively. Experimental rates are depicted as are theoretical rates and theoretical amplitudes. However, since the data are still in a preliminary stage, a definitive fit is not possible and awaits the more detailed analysis of the raw data by Fleming's group. For longitudinal fields, the preliminary theoretical fitted relaxation rates are depicted by the solid line in Fig. 1. The dashed line is the relaxation rate of the next lowest mode having significant contribution to the signal and the dash-

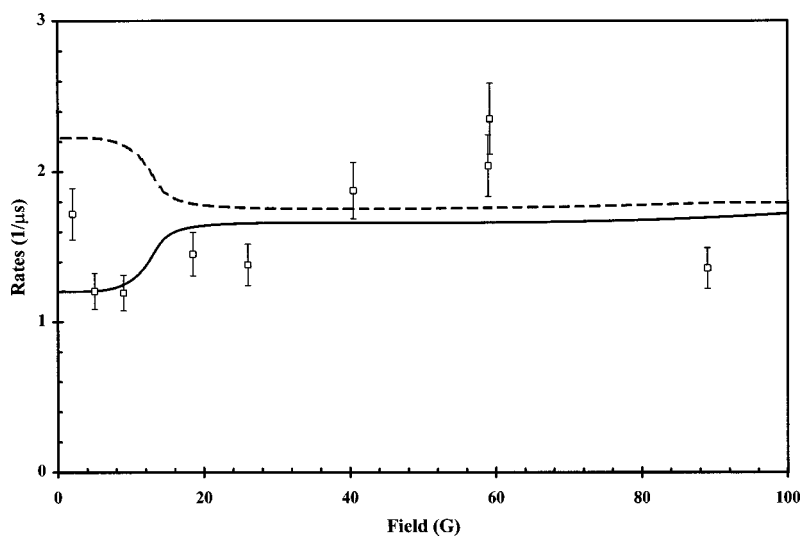


FIG. 3. Experimental transverse muon spin relaxation rate versus magnetic field at a total pressure of 351.0 atm. The squares are the lowest-frequency experimental data points with estimated errors for a CO pressure of 0.0036 atm, while the solid curve is the fit. The dashed curve is the predicted relaxation rate for the higher-frequency mode.

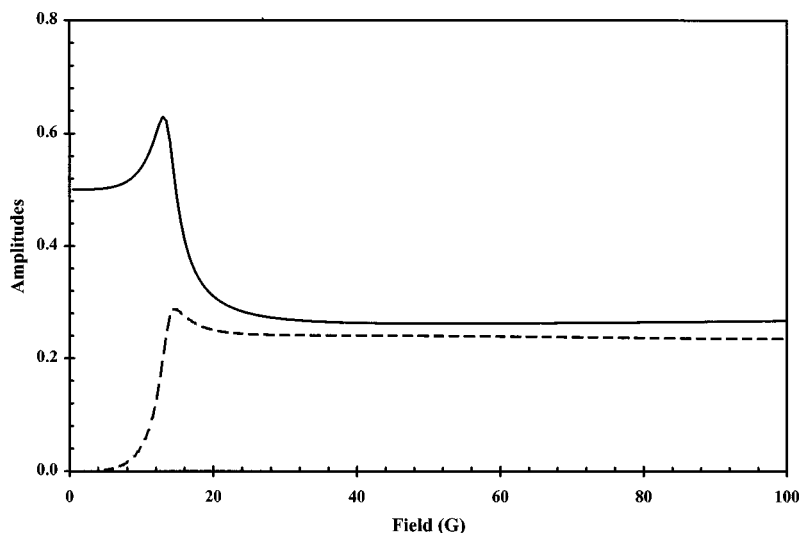


FIG. 4. Predicted transverse amplitudes. The solid curve is the amplitude of the lowest-frequency mode, while the dashed curve is the amplitude of the second lowest-frequency mode.

dotted line is the third lowest. Predicted amplitudes for these modes are given in Fig. 2. That is, these lines represent those modes with appreciable muon amplitudes that have the three lowest relaxation rates. Since the preliminary fit appears to be reasonable, it is suggested that the raw data be reanalyzed with at least two exponentially decaying relaxation modes present. For transverse fields, the preliminary theoretical fit to the data suggests that the relaxation rate associated with the higher of the two frequencies is larger over the depicted field region than the lower-frequency relaxation rate. However, for intermediate fields where the frequencies can be distinguished, the theory predicts that the relaxation rates are within experimental uncertainty of each other. On the other hand, for lower fields ( $\leq 30$  G) where the frequencies are not easily resolvable or not resolvable at all, the preliminary theoretical fit suggests that the two exponential decay rates are sufficiently different that they should be resolvable and that two exponential modes should be present. However, the amplitude of the largest relaxation rate rapidly approaches zero with decreasing field and the range where the two different relaxation rates should be resolvable might be small. Only reanalysis of the raw experimental data will confirm or deny these theoretical predictions based upon the present preliminary fit.

Although the fit is preliminary, it is still possible to make rough comparisons with data for the relatively well studied HCO radical; see Table II. The reaction rate of hydrogen and carbon monoxide with an argon moderator has been studied, with the value [34] for the third-order rate constant  $k_o$  as given in Table II. For the current fit a comparable rate constant is given by the ratio of the product of the forward binary rate and the sum of the stabilization rate and the rotational relaxation rate divided by the unimolecular decay rate

$$k_0 = \frac{k_{fb}(k_s + k_1)}{k_r}. \quad (77)$$

The value for MuCO determined in this way (see Table II) is a factor of 22 larger than the HCO rate. As this pseudo-third-order rate is constructed from the product of bimolecular rates divided by a unimolecular rate, it should be inversely

proportional to the reduced mass of the proton or the muon. Thus, if the difference in isotopes is only due to this product of collision frequencies, then the MuCO rate would be 9 times the HCO rate. The current preliminary fit thus suggests that there are further effects with muonium that speed up the reaction. Clearly, a difference in tunneling probability could be involved, but it should also be stated that the present fitting values are based on an interpretation of how the muon spin is affected during the chemical reactions rather just on the numbers of molecules that react. It is also of interest to note that this pseudo-third-order rate is equal, within uncertainties, to the fitted third-order rate  $k_{ft}$  that was required for a reasonable fit. This gives further justification for the inclusion of the third-order reaction mechanism when describing the spin dynamics. Another comparison that may be made is with the isotropic hyperfine constant  $\omega_0$ . Both experimental HCO [35] and theoretical MuCO [36] values exist; see Table II. Thus the current fitted MuCO value is less than the theoretical MuCO [36] value by a factor of 2.3. Since the current result is preliminary and the term in the Hamiltonian associated with this parameter depends upon neither the field nor pressure, such a result is not unreasonable. Finally, the spin rotation constant  $\omega_{SR}$  for MuCO is compared with that for HCO. For HCO, the components of the anisotropic spin rotation tensor are listed in [35], but approximating HCO as a diatomic molecule, as is done in the present paper for MuCO, it is appropriate to average only those tensor components that are associated with directions perpendicular (roughly) to the CO axis; compare the leading term of Eq.

TABLE II. Comparison to HCO data.

Parameter	HCO (experiment)	MuCO (present fit)	MuCO (theory)
$\omega_0$ (rad/ $\mu$ s)	2337.0 <sup>a</sup>	3830.0	8760.0 <sup>b</sup>
$\omega_{SR}$ (rad/ $\mu$ s)	-589.0 <sup>c</sup>	-85.0	
$k_0$ (cm <sup>6</sup> /s)	$1.54 \times 10^{-34}$ <sup>d</sup>	$33.6 \times 10^{-34}$	
$k_{ft}$ (cm <sup>6</sup> /s)		$35.3 \times 10^{-34}$	

<sup>a</sup>Reference [35].

<sup>b</sup>Reference [36].

<sup>c</sup>References [35,37].

<sup>d</sup>Reference [34].

(6) in Ref. [37]. That is the literature value listed in Table II. Thus, while preliminary, the fitted values of the parameters are of the order of what would be expected based upon hydrogen atom data.

While the preliminary nature of the experimental data and the various approximations made for the collisional spin dynamics do not allow a definitive evaluation of the spin coupling parameters and reaction rate constants to be made, the theoretical treatment of the chemically reacting, spin relaxing system is presented here as a methodology of approach. While its apparent ability to fit experiment helps to justify the method of approach, the mechanism of the chemical reaction scheme needs to be better understood. A better understanding of the detailed spin transition rates during a chemical reaction is also needed. In particular, the product of the exchange reaction has been labeled as a stable species, yet the contribution of this species to determine the relaxation-precession modes has been included. In contrast, the stabiliza-

tion of the bimolecularly produced metastable radical yields a stable species that is not included. Possibly the former product is a metastable radical in a different excited state so its subsequent reactions are different. On the other hand, possibly a stabilization reaction is sufficiently disruptive that it causes a loss of coherence of the spin polarization, whereas the bimolecular addition and exchange reactions allow a preservation of the spin polarization. While a number of alternate reaction schemes were tried, it is the above-described fitting procedure that gave the best fit. It is a rationalization of this reaction scheme that has been given.

#### ACKNOWLEDGMENTS

This work was supported in part by the Natural Sciences and Engineering Research Council of Canada. The authors thank Dr. Fleming, Dr. Arseneau, and Dr. Pan for access to their experimental data and for various discussions regarding the data and the chemistry of the Mu-CO system.

- 
- [1] Proceedings of the 7th International Conference on Muon Spin Rotation/Relaxation/Resonance ( $\mu$ SR'96), Part III, edited by K. Nagamine, R. M. Macrae, R. Kadono, and K. Nishiyama [Hyperfine Interact. **106** (1997)].
- [2] D. C. Walker, *Muon and Muonium Chemistry* (Cambridge University Press, Cambridge, 1983).
- [3] A. Schenck, in *Muon Spin Rotation Spectroscopy: Principles and Applications in Solid State Physics* (Hilger, Bristol, 1985).
- [4] D. M. Garner, Ph.D. thesis, University of British Columbia, 1979 (unpublished); A. C. Gonzalez *et al.*, J. Chem. Phys. **91**, 6164 (1989); **97**, 6309 (1992).
- [5] J. J. Pan, Ph.D. thesis, University of British Columbia, 1996 (unpublished).
- [6] D. Arseneau, J. J. Pan, M. Senba, M. Shelly, and D. G. Fleming, Hyperfine Interact. **106**, 151 (1997).
- [7] M. Senba, D. G. Fleming, D. J. Arseneau, D. M. Garner, and I. D. Reid, Phys. Rev. A **39**, 3871 (1989).
- [8] R. J. Mikula, Ph.D. thesis, University of British Columbia, 1981 (unpublished).
- [9] D. G. Fleming, R. F. Kiefl, D. M. Garner, M. Senba, A. C. Gonzalez, J. R. Kempton, D. J. Arseneau, K. Venkateswaran, P. W. Percival, J. C. Brodovitch, S. K. Leung, D. Yu, and S. F. J. Cox, Hyperfine Interact. **65**, 767 (1990).
- [10] J. J. Pan, D. G. Fleming, M. Senba, D. J. Arseneau, R. Snooks, S. Baer, M. Shelley, P. W. Percival, J. C. Brodovitch, B. Addison-Jones, S. Wlodek, and S. F. J. Cox, Hyperfine Interact. **87**, 865 (1994).
- [11] D. G. Fleming, J. J. Pan, M. Senba, D. J. Arseneau, R. F. Kiefl, M. Y. Shelly, S. F. J. Cox, P. W. Percival, and J. C. Brodovitch, J. Chem. Phys. **105**, 7517 (1996).
- [12] D. G. Fleming, D. M. Garner, L. C. Vaz, D. C. Walker, J. H. Brewer, and K. M. Crowe, Adv. Chem. Ser. **175**, 279 (1979).
- [13] D. G. Fleming and M. Senba, in *Perspectives of Meson Science*, edited by T. Yamazaki, N. Nakai, and K. Nagamine (North-Holland, Amsterdam, 1992), pp. 219–264.
- [14] D. J. Arseneau, Ph.D. thesis, University of British Columbia, 1992 (unpublished).
- [15] D. G. Fleming, M. Senba, D. M. Garner, R. J. Mikula, and D. J. Arseneau, Chem. Phys. **82**, 75 (1983).
- [16] R. E. Turner, R. F. Snider, and D. G. Fleming, Phys. Rev. A **41**, 1505 (1990).
- [17] M. Senba, Phys. Rev. A **50**, 214 (1994).
- [18] M. Senba, Phys. Rev. A **52**, 4599 (1995).
- [19] R. E. Turner and R. F. Snider, Phys. Rev. A **50**, 4743 (1994).
- [20] R. E. Turner and R. F. Snider, Phys. Rev. A **54**, 4815 (1996).
- [21] R. J. Duchovic, A. F. Wagner, R. E. Turner, D. M. Garner, and D. G. Fleming, J. Chem. Phys. **94**, 2794 (1991).
- [22] A. Abragam, *The Principles of Nuclear Magnetism* (Oxford University Press, Oxford, 1961).
- [23] E. Roduner, in *The Positive Muon as a Probe in Free Radical Chemistry*, edited by G. Berthier, M. J. S. Dewar, H. Fischer, K. Fukui, G. G. Hall, J. Hinze, H. H. Jaffé, K. Ruedenberg, and J. Tomasi, Lecture Notes in Chemistry Vol. 49 (Springer, Berlin, 1988).
- [24] B. D. Patterson, Rev. Mod. Phys. **60**, 69 (1988).
- [25] I. I. Rabi, Phys. Rev. **51**, 652 (1937).
- [26] R. E. Turner, Phys. Rev. A **28**, 3300 (1983); R. E. Turner and M. Senba, *ibid.* **29**, 2541 (1984); J. Chem. Phys. **84**, 3776 (1986).
- [27] D. G. Fleming (private communication).
- [28] L. Waldmann, Z. Naturforsch. A **12**, 660 (1957).
- [29] R. F. Snider, J. Chem. Phys. **32**, 1051 (1960); Int. Rev. Phys. Chem. **17**, 185 (1998).
- [30] B. C. Sanctuary and R. F. Snider, J. Chem. Phys. **55**, 1555 (1971).
- [31] J. A. R. Coope and R. F. Snider, J. Math. Phys. **11**, 1003 (1970).
- [32] J. A. R. Coope, J. Math. Phys. **11**, 1591 (1970).
- [33] A. R. Edmonds, *Angular Momentum in Quantum Mechanics* (Princeton University Press, Princeton, 1960).
- [34] D. L. Baulch *et al.*, J. Phys. Chem. Ref. Data **23**, 847 (1994).
- [35] W. Weltner, Jr., *Magnetic Atoms and Molecules* (Van Nostrand Reinhold, New York, 1983).
- [36] B. C. Webster, J. Chem. Soc., Faraday Trans. **93**, 205 (1997).
- [37] C. C. Lin, Phys. Rev. **116**, 903 (1959).